JOURNAL OF MAPS, 2017
VOL. 13, NO. 2, 260–269
http://dx.doi.org/10.1080/17445647.2017.1296790

SCIENCE

OPEN ACCESS

Geomorphology of Ius Chasma, Valles Marineris, Mars

Krzysztof Dębniak [a], Daniel Mège [b,c,d] and Joanna Gurgurewicz [a,b]

[a]Institute of Geological Sciences, Polish Academy of Sciences, Research Centre in Wrocław, Wrocław, Poland; [b]Space Research Centre, Polish Academy of Sciences, Warsaw, Poland; [c]Laboratoire de Planétologie et Géodynamique, UMR CNRS 6112, Université de Nantes, Nantes, France; [d]Observatoire des Sciences de l'Univers Nantes Atlantique, Nantes, France

ABSTRACT

Cartographic products of the Martian trough system, Valles Marineris, are useful to identify the diversity and complexity of geological activity that has occurred there. A huge fraction of the processes that have shaped the surface of Mars are also concentrated there. A geomorphological map of Ius Chasma in western Valles Marineris is presented. The map is published in three sheets at 1:260,000. It was drawn on the basis of 100 Mars Reconnaissance Orbiter's Context Camera images of 12 m/pixel resolution, mosaiced using the USGS ISIS Planetary Image Processing Software, and subsequently mapped and interpreted for geomorphology in ArcGIS. The map displays 52 main geomorphological units of which some are further subdivided. They include both well-established features (e.g. spur-and-gully morphology on trough walls, landslide scars, and deposits), and newly reported landforms (e.g. alluvial fans with dendritic channels, moraines in western Ius Chasma). The proposed classifications of landslide deposits, glacial landforms, and floor areas are more detailed than on any previous map of Valles Marineris. The Ius Chasma map is the first cartographic product presenting a full inventory of dune fields, impact craters, light-toned outcrops, and mass-wasting features.

ARTICLE HISTORY
Received 25 April 2016
Revised 10 February 2017
Accepted 15 February 2017

KEYWORDS
Valles Marineris; Mars; ArcGIS; ISIS; mapping; geomorphology

1. Introduction

The Valles Marineris trough system on Mars is composed of 12 deep, steep-sided, elongated chasmata which have experienced multiple geological processes since their formation ~4 Ga. Structural, magmatic, fluvial, lacustrine, glacial, and eolian processes, landsliding and impact cratering shaped the walls and floors of Valles Marineris and thus are excellent indicators of past conditions on Mars and their evolution through time.

Valles Marineris was discovered during a dust storm in 1971 by the NASA Mariner 9 orbiter. Since then, the investigation of chasmata have revealed numerous landforms and led to the publication of several geological and geomorphological maps. Valles Marineris is presented in geological maps of Mars at small scale, 1:15,000,000 (Scott & Tanaka, 1986) and 1:20,000,000 (Tanaka et al., 2014). Geological maps of the entire system were prepared by McCauley (1978) at a scale of 1:5,000,000, followed by a map prepared on two sheets at 1:2,000,000 (Witbeck, Tanaka, & Scott, 1991). The detailed maps of full, individual troughs were made for Ophir and Central Candor Chasmata (Lucchitta, 1999), and Melas Chasma (Peulvast, 1991; commented in Peulvast & Masson, 1993a, 1993b), at a scale of 1:500,000. While the latter is the most detailed cartographic publication showing a significant part of Valles Marineris from a geomorphological perspective, the first contains valid classifications of floor, landslide, and Interior Layered Deposit units which were used as a starting point for this publication.

Valles Marineris mapping also benefits from many other contributions, such as studies of (*1*) wall types and tectonic features (Peulvast, Mège, Chiciak, Costard, & Masson, 2001), (*2*) ages and characteristics of landslides (Quantin, Allemand, & Delacourt, 2004; Quantin, Allemand, Mangold, & Delacourt, 2004), (*3*) landslide geomorphological inventory in Ius and Tithonium Chasmata (Brunetti et al., 2014), (*4*) geological units in central Ius Chasma (Mège & Bourgeois, 2011), Capri and Eos Chasmata (Flahaut, Quantin, Allemand, Thomas, & Le Deit, 2010), western Melas Chasma (Pelkey, Jakosky, & Christensen, 2003), and Hebes Chasma (Jackson, Adams, Dooley, Gillespie, & Montgomery, 2011), (*5*) glacial features in Ius, Candor, and Capri Chasmata (Gourronc et al., 2014), (*6*) dendritic channel systems in the Melas basin and the Echus plateau (Mangold, Ansan, Masson, Quantin, & Neukum, 2008; Mangold, Quantin, Ansan, Delacourt, & Allemand, 2004; Quantin, Allemand, Mangold, Dromart, & Delacourt, 2005), (*7*) structural features in southwest Candor

CONTACT Krzysztof Dębniak krzysztof.debniak@twarda.pan.pl Institute of Geological Sciences, Polish Academy of Sciences, Research Centre in Wrocław, Podwale 75, Wrocław 50-449, Poland

Chasma (Okubo, 2010; Okubo, Lewis, McEwen, & Kirk, 2008), (*8*) morphostructural analysis in Melas Chasma (Peulvast & Masson, 1993a, 1993b), (*9*) mineralogical characteristics in several chasmata (Chojnacki & Hynek, 2008; Fueten, Flahaut, Stesky, Hauber, & Rossi, 2014; Roach, Mustard, Lane, Bishop, & Murchie, 2010; Roach, Mustard, Swayze, et al., 2010; Wendt et al., 2011), (*10*) sand dune fields in most Valles Marineris chasmata (Chojnacki, Burr, & Moersch, 2014; Chojnacki, Burr, Moersch, & Wray, 2014; Chojnacki, Moersch, & Burr, 2010), and (*11*) Light-toned Layered Deposits (LLDs) on plateaus near Juventae and Ganges Chasmata (Le Deit et al., 2010).

The production of detailed geomorphological maps of Valles Marineris chasmata is now possible at a scale of ~10 m. Twenty successful missions to Mars delivered information from the Martian surface, including orbital imagery and spectral data. Over time, the resolution of images has significantly increased from ~1 km for the Mariner missions in the 1960s and 1970s to 25 cm/pixel for the High Resolution Imaging Science Experiment camera, HiRISE, onboard Mars Reconnaissance Orbiter since 2006 (McEwen et al., 2007). The improvements of computational capabilities in the last two decades have made mapping possible for large areas of Mars with increasing accuracy, from a resolution of 150–300 m/pixel by the Viking orbiter cameras (William, 2016) to 6 m/pixel for the Mars Reconnaissance Orbiter's Context Camera, CTX (Malin et al., 2007). A diverse set of geomorphological features are present in Ius Chasma and are the research topic for this map.

The prepared geomorphological map of Ius Chasma is based on the authors' interpretations, interpretations reported in earlier studies conducted in Ius Chasma, and interpretations of similar features recognized in other Valles Marineris chasmata.

2. Study area

Valles Marineris is a system of elongated depressions (chasmata) over 3100 km long from the western boundary with Noctis Labyrinthus to the eastern area where it meets chaotic terrains. In spite of intense geomorphological reworking, chasma initiation itself involved tectonic processes. It has been suggested on the basis of surrounding coeval grabens (Schultz, 2000), produced by rifting in response to Tharsis plume evolution (Mège & Masson, 1996a) and associated magmatic loading (Banerdt & Golombek, 2000). The location of Valles Marineris might have been influenced by the changing lithosphere structure within the Martian dichotomy boundary (Andrews-Hanna, 2012). Valles Marineris is divided into 12 troughs (Figure 1), of which 7 are interconnected (Ius, Ophir, Candor, Melas, Coprates, Capri, and Eos Chasmata) via the central area, 2 are connected to the others from the west via Noctis Labyrinthus (Tithonium Chasma) and the east via the chaotic terrains (Ganges Chasma), 1 is closed (Hebes Chasma), and 2 are directly open to the northern Martian plains via outflow channels (Echus and Juventae Chasmata). The cumulative length of all individual chasmata exceeds 6400 km. Trough width ranges from ~10 km in the narrowest parts of Tithonium Chasma to ~290 km in Melas Chasma and ~390 km in the Capri-Eos area. Trough depths range from a few kilometers in Echus and Tithonium Chasmata to approximately 10 km in Candor and Coprates Chasmata. The entire Valles Marineris system covers an area of more than 760,000 km^2, comparable to the size of Chile. The geological history of Valles Marineris is almost as long as the geological history of Mars, starting at the end of the Noachian at ca. 4.0 Gy (Carr & Head III, 2010).

2.1. Ius Chasma

Ius Chasma is connected with Noctis Labyrinthus in the west, Melas Chasma in the east, bordered by Sinai Planum in the south, and aligned with Tithonium Chasma located to the north. It is a tectonic-controlled depression of ~850 km in length, width up to 120 km in width, and depth locally exceeding 8 km. Ius Chasma is composed of two parallel, E–W trending valleys separated by the Geryon Montes ridge (see Context map in the Western Section of the geomorphological Main Map), ~5 km high and up to 26 km wide. The Ius Chasma floor elevation decreases to the east, toward Melas Chasma (Gourronc et al., 2014). Some of the most characteristic geomorphological features related to the chasma are sapping channel systems (Louros Valles, see Context map), large landslides (Brunetti et al., 2014), spur-and-gully wall morphology (Peulvast et al., 2001), and LLDs on the plateau south of the trough (Weitz et al., 2010).

A large portion of Ius Chasma formed by the connection of grabens (Blasius, Cutts, Guest, & Masursky, 1977; Frey, 1979; Masson, 1977; Mège & Masson, 1996b; Peulvast et al., 2001; Schultz, 1995, 1998). Syntectonic erosion gave birth to a spur-and-gully morphology on chasma walls, some of which were later reactivated by channelized flows, modified by glacial erosion (e.g. Mège & Bourgeois, 2011), and removed by mass-wasting processes (e.g. Brunetti et al., 2014) and sapping channels (e.g. Kochel & Piper, 1986; Lucchitta et al., 1992).

Although it has been agreed that the topography in Ius Chasma is largely the result of tectonic stretching, the formation of the spur-and-gully morphology itself has been debated, with competing hypotheses as diverse as water incision, submarine or sublacustrine currents, or granular flows (Lucchitta et al., 1992).

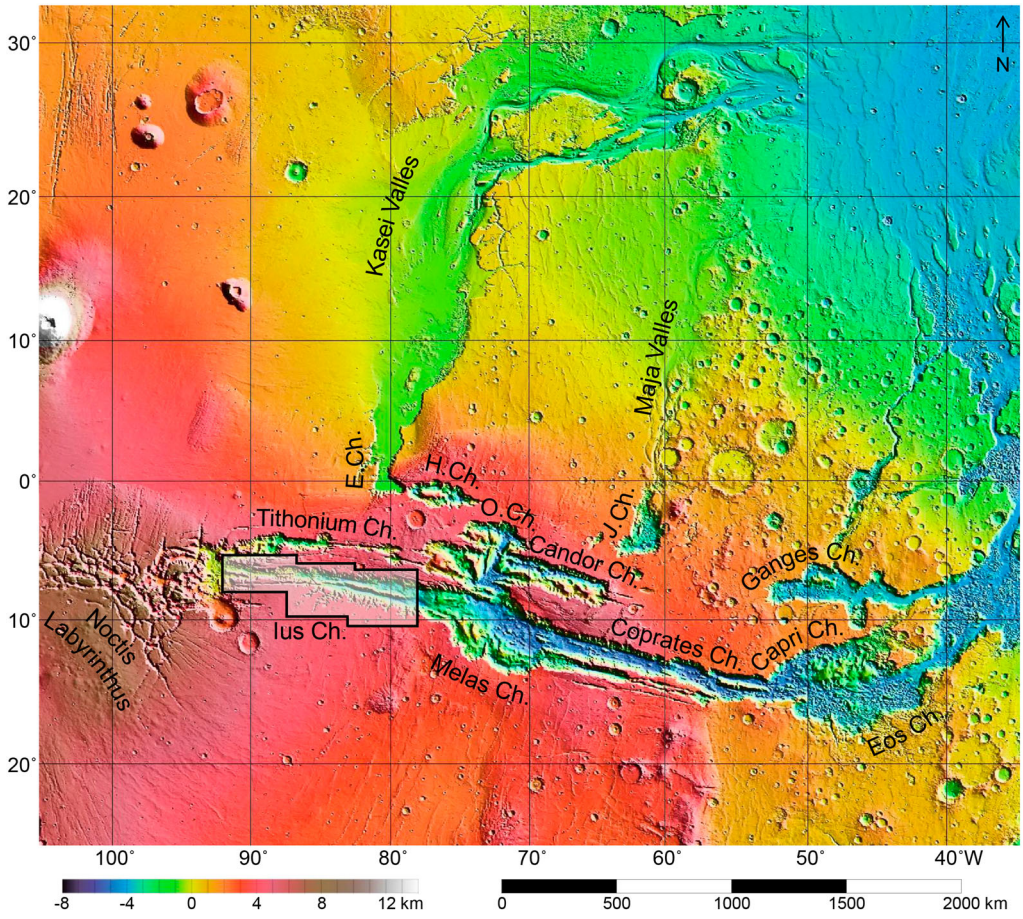

Figure 1. Topographic map of Valles Marineris area from Mars Orbiter Laser Altimeter (NASA/MGS/MOLA Science Team). Area covered by the geomorphological map marked in polygon. Distance bar scale legit for the equator. *Abbreviations:* Ch. – Chasma, E.Ch. – Echus Chasma, H.Ch. – Hebes Chasma, J.Ch. – Juventae Chasma, O.Ch. – Ophir Chasma.

This morphology is visible in Geryon Montes and on chasma walls, but only in places where it has not been destroyed by later formation of sapping channels and landslides. Therefore, landslides might be too young to allow the spur-and-gully morphology formation, or this morphology developed in an early, probably wetter, environment (Lucchitta et al., 1992).

Water erosion probably participated in spur-and-gully formation, but also generated sapping channels on both chasma sides. The largest sapping channel system (Louros Valles) is located south of the chasma and consists of channels of individual lengths in the range of 30–130 km. Sapping channels were probably active up to the Early Amazonian (Craddock & Howard, 2002). They cut spur-and-gully morphology (Peulvast et al., 2001). The last group of large-scale processes in Ius Chasma involves landslides. Their deposits cover much of the chasma floor. Episodic landslide activity accompanied the Ius Chasma history from initial rifting to the recent times (Quantin, Allemand, Mangold, et al., 2004).

3. Data, software, and methods

The Main Map of Ius Chasma was prepared on the basis of CTX images. The imagery dataset was processed and mosaiced. The prepared map includes all geomorphological features within the chasma that can be observed at the resolution of 12 m/pixel.

3.1. Data

CTX images were used to create the background mosaics for geomorphological mapping. One hundred panchromatic CTX images with an original spatial resolution of 6 m/pixel and width up to 30 km (Malin et al., 2007) were obtained from the Mars Orbital Data Explorer website (NASA PDS Geoscience Node) and subsequently processed and mosaiced with Integrated Software for Imagers and Spectrometers, ISIS (Gaddis et al., 1997). The spatial resolution of resultant images was decreased to 12 m/pixel in order to optimize the mapping procedure in Esri ArcGIS. HiRISE images provide discontinuous coverage at the higher spatial resolution of up to 25–32 cm/pixel (Ebben, Bergstrom, Spuhler, Delamere, & Gallagher, 2007), and were incorporated into the project as a supplementary dataset in order to verify interpretations of ambiguous areas. HiRISE images include a broad, panchromatic band as well as three narrower spectral bands in the infrared, red, and blue acquired in a ~1 km strip embedded within a ~5 km wide

panchromatic image of variable length. HiRISE images therefore allow us to refine CTX-based observations locally and improve interpretations. The investigated area of Ius Chasma contained 207 HiRISE images when this work was conducted.

Mars Global Surveyor's Mars Orbiter Laser Altimeter data, MOLA, provided topographic information with an accuracy of ~30 m and a spatial sampling of ~300 m (Smith et al., 2001; Zuber et al., 1992), enabling easier separation of some geomorphological features and identification of some processes. Topography data were important for mapping the floor/wall transition in Valles Marineris and subtle changes in chasma floor units.

3.2. Software and methods

The mapping procedure was conducted in three different programs corresponding to three stages of activities: (*1*) Java Mission-planning and Analysis for Remote Sensing, JMARS (Christensen et al., 2009) – collecting CTX images; (*2*) Integrated Software for Imagers and Spectrometers, ISIS (isis.astrogeology.usgs.gov) – modifying and mosaicing CTX images; and (*3*) ArcGIS (Environmental Systems Research Institute, 2011) – incorporating CTX mosaics, HiRISE images and MOLA data, and performing the actual mapping procedure.

JMARS is a geospatial information system developed by Arizona State University's Mars Space Flight Facility to provide mission planning and data analysis tools. JMARS was used to generate a spatial dataset as a CTX image stamp map. The required images of western Valles Marineris were identified in JMARS and acquired from the Mars Orbital Data Explorer website.

ISIS, developed by the USGS Astrogeology Research Program, has been a basic tool for the cartographic and scientific analysis of planetary images since 1992 (with previous software versions reaching back to 1971). The major ISIS applications have the ability to precisely control planetary data, and to calculate the location and orientation of the observer and the target by putting pixels in the correct location in digital space. ISIS is used to process images acquired in most Martian, lunar, and other Solar System missions ever performed by NASA. In the current work, ISIS was used as a tool for the CTX image mosaic preparation. The mosaicing procedure was divided into 18 steps (Figure 2).

The initial CTX image transformations were performed by four ISIS applications: *mroctx2isis* (which imports an CTX image as an ISIS cube), *spiceinit* (which updates SPICE data, such as kernels, pointing, and position, for a camera cube), *ctxcal* (which radiometrically calibrates a CTX image, for example, removes a *smile effect*), and *ctxevenodd* (which removes even/odd detector striping from CTX images – first level of calibration, *lev1*). Afterwards, the list of *lev1* images was prepared in order to implement it in the application used in the next step: *maptemplate* (which creates a map file template PVL containing the mapping group keywords required to transform an image to a map projection; this application was used once only). In the *maptemplate* processing stage, the following options were selected: projection – sinusoidal, latitude type – planetocentric, longitude direction – positive east, longitude domain – from −180° to 180°, resolution – MPP 12. The *cam2map* application was subsequently used to convert the camera image to a map projection by implementing the PVL file (second level of calibration, *lev2*). Two additional image lists were prepared next: a list of *lev2* images and a list containing only one *lev2* image, the one that is of highest general quality (i.e. displaying good

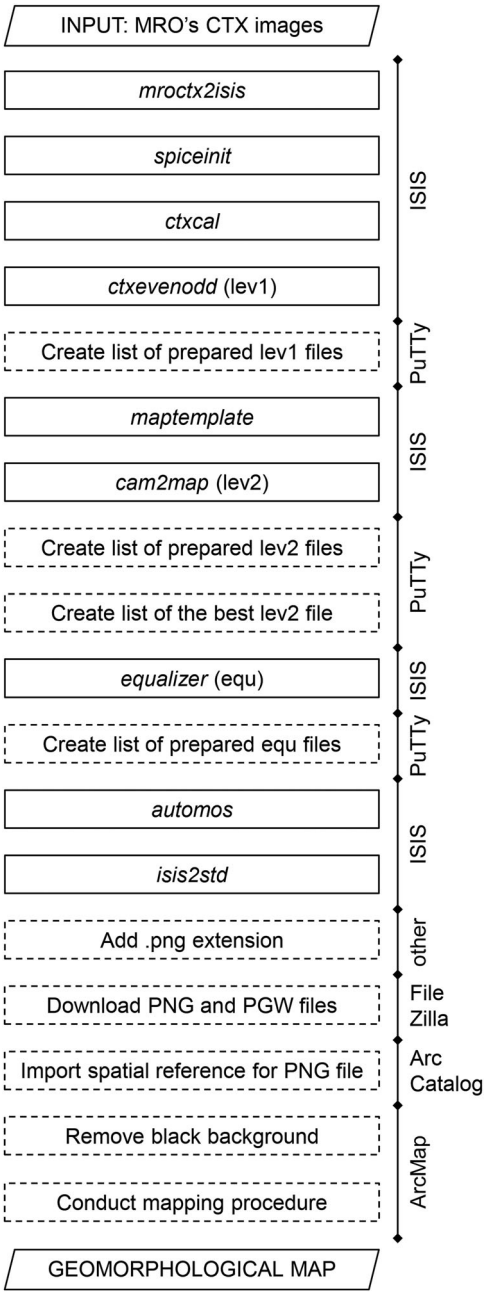

Figure 2. Scheme of mosaic and map preparation procedure.

sharpness, lack of bad pixels). Both lists were used in the subsequent step in *equalizer* (which matches tones of the projected cubes). The final list of images, produced by *equalizer*, was formed and subsequently entered in the *automos* application (which creates a mosaic using a list of map projected cubes). The resulting cube was then exported by *isis2std* to a final ISIS file, to which the '.png' extension was added. The PNG file and corresponding world file (PGW) were downloaded from the server by FileZilla, adjusted in Esri ArcCatalog (spatial reference was imported from the CUB file produced in *automos*), and initially processed in ArcMap by removing the black image background. The mosaic was then ready for geomorphological mapping. The Ius Chasma map was produced in GCS Mars 2000 Sphere coordinate system and plate carrée projection (equirectangular projection).

ISIS allows the generation of useable image mosaics but the program has two significant file size limitations: 12 GB for *automos*, and 2 GB for *isis2std*. If the input file is too large, mosaic production will not be completed. The mosaic file size does not depend on the number of individual images included in the mosaic, but rather the area covered by the final mosaic. Therefore, the set of images from a study area should be carefully divided into smaller subsets. In this work, 100 images from the region of Ius and Tithonium Chasmata have been arranged in to three subsets in order to produce satisfactory mosaics. The western, central, and eastern mosaics differ in size, covered area, and the number of included images (Figure 3 and Table 1).

The mapping procedure was performed in Esri ArcGIS, a geographic information system designed for map production, data compilation, and mapped information analysis.

4. Results

The units marked on the geomorphological map of Ius Chasma cover an area of 86,048 km^2 and contain 52 symbols, including:

- 7 main units constituting the essence of the map and covering most of the mapped area (i.e. spur-and-gully morphology, sapping channels, pit chains, large landslide scars, large landslide deposits, glacial features, and floor units),
- 20 supplementary units emphasizing the diversity of landforms in Ius Chasma (i.e. isolated buttes, higher benches, lower benches, basal escarpments, valley infills, collapsed wall rocks, tongue-shaped feature, small landslides, major talus cones, bright material, scarps, periodic bedrock ridges, ridged unit, rounded floor unit, alluvial plain, black dune fields,

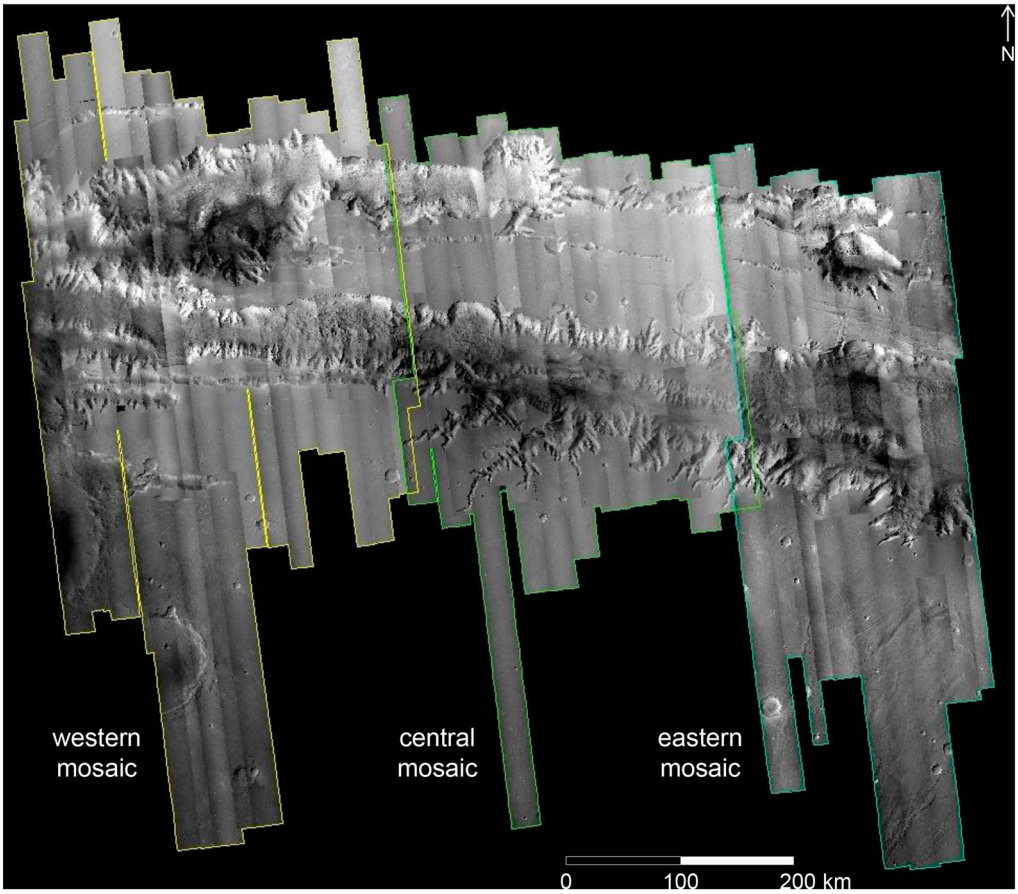

Figure 3. CTX image mosaics prepared in ISIS for Ius Chasma mapping.

Table 1. The summary of CTX image mosaics produced by ISIS software.

Mosaic	Mosaic area (km^2)	Number of incorporated CTX images	Cumulative size of all individual CUB files (after *equalizer*)	Size of final CUB mosaic file (after *automos*)	Size of final PNG mosaic file
Western	159 886	46	26.55 GB	6.10 GB	1.96 GB
Central	108 034	29	17.80 GB	6.59 GB	1.64 GB
Eastern	107 241	25	17.87 GB	6.02 GB	1.50 GB

sand covers, regular dune fields, light-toned outcrops, and large craters),
- 25 other units and symbols presenting details of the geomorphological environment of the trough (i.e. boulders, flat plates, chasma rim, retreated upper wall slopes, LLDs on the plateau surrounding Valles Marineris, crest lines, scarps, trimlines and related fallen rocks, normal faults, exhumed fractures, fractures undifferentiated (marked as *fractures (other)* in the map), depressions, channels, craters, leakages, knobs, examples of bedrock layering, directions of wall material movements and large landslide grooves, sharp edges within landslide deposits, other mass movements, and three wall types).

Ius Chasma hosts numerous well-studied Valles Marineris morphologies, including spur-and-gully (Peulvast et al., 2001), sapping channels (Higgins, 1982), and landslides (Brunetti et al., 2014; Quantin, Allemand, & Delacourt, 2004; Quantin, Allemand, Mangold, et al., 2004), mapped with unprecedented precision. The prepared legend of the Geomorphological Map of Ius Chasma contains three major sections which were distinguished on the basis of unit locations, that is, (1) wall-related features, (2) mass movement-related features, and (3) floor-related features, and an additional major section containing (4) other landforms and features. The only section of strictly genetic characteristics is the one regarding mass movements, while the others contain features and landforms of various origin. For example, glacial-related features can be found in two major sections, that is, higher benches in Wall-related features, and moraines in Floor-related feaures. The proposed legend division makes the map easy to navigate and work with. The map conveys several new types of information which are presented below.

4.1. Wall-related features

Wall-related units are represented by features of different origin which are present within Ius Chasma walls (except for features related to mass movements which are classified in a separate major section).

(1) Wall morphology is divided into three types: active (uncratered slope surfaces showing evidence of slope movements), grooved (displaying parallel grooves of inferred creeping origin), and inactive (appearing as the surface of a material having enough strength for bowl-shaped crater morphology to be stable on slopes).

(2) Most of the walls of Ius Chasma and its internal ridge display spur-and-gully morphology which covers an area of 24,792 km^2.

(3) Sixty-six sapping channels are present in Ius Chasma, including well-developed sapping channels in the central chasma, single channels in western and eastern areas of the trough, and remnants of sapping channels cut and removed by mass movements. Sapping channels are strongly controlled by brittle tectonic structures (e.g. Sharp & Malin, 1975), presented as *exhumed fractures* on the map.

(4) Glacial landforms observed within walls are present in central and eastern parts of the trough. Basal escarpments, trimlines, and higher benches are probable relicts of glacier ice and were already partially reported in Gourronc et al. (2014) and Mège and Bourgeois (2011).

4.2. Mass movement-related features

Mass movements led to the production of several types of landforms, among which large landslides are the most visible manifestation of gravity-driven processes.

(5) Ius Chasma hosts 21 large landslide scars and almost 23,000 km^2 of mass-wasting deposits related to large-scale mass movements. These deposits are divided into 10 geomorphological types.

(6) The prepared map of Ius Chasma contains also over 1100 other features resulting from mass movements, including collapsed wall rocks, small landslides, talus cones, a tongue-shaped feature, and bright-toned, probably old landslide deposits. All of them imply intense slope activity in Ius Chasma during various periods.

4.3. Floor-related features

The section of floor-related features contains landforms not obliterated by landslide deposits. This section is divided into two geomorphological groups (i.e. glacial features and floor units) and six individual units, including alluvial plains.

(7) Glacial features, dominated by accumulation landforms, occur in the western part of the trough. Terminal and ground moraines, till plains,

outwash plains, and patterned ground are reported in this region for the first time.

(8) There are nine divisions in the floor units' group. Four of them are composed of light-toned deposits of possible aqueous origin (Flahaut et al., 2012; Roach, Mustard, Lane, et al., 2010; Roach, Mustard, Swayze, et al., 2010b). The westernmost part of the southern Ius graben (central sheet, 84°05′–84°45′W) displays flat floor deposits, locally carved into outcrops revealing light-toned deformed materials (Metz, Grotzinger, Okubo, & Milliken, 2010). The area is surrounded by a lower bench located near the walls. The bench may be a relic of deposits from a past lake or pond. Neighboring debris aprons appear as smoothened by water activity, suggested by the aqueous origin of surrounding landforms.

(9) Three alluvial plains in the southern Ius graben were incised by dendritic, branched channels. River networks have already been recognized in Melas Chasma (Metz et al., 2009), near Echus Chasma (Mangold et al., 2004), and in one location in Ius Chasma (Mège & Bourgeois, 2011), but two other alluvial plains in Ius Chasma have not been reported before.

4.4. Other landforms and features

The map also presents other geomorphological features, among which light-toned outcrops, dunes, and impact craters are the most abundant, and slope leakages are reported for the first time.

(10) Bright layered deposits are frequent on chasma slopes and in landslide deposits (light-toned outcrops unit in the map) implying a series of distinct aqueous events in Ius Chasma in the past. Although fluvial activity was proposed in Roach, Mustard, Swayze, et al. (2010b) to explain the widespread occurrence of water-related minerals in Ius Chasma, the map reveals a lacustrine-ponding environment and groundwater discharges in relation to the deposition of light-toned materials, as discussed below. On slopes, these deposits are frequently visible in outcrops affected by mass movements of surface materials. The geomorphological map contains nine major occurrences, locally associated with mild deposits appearing as products of fluidized slides. This association is in agreement with an aqueous hypothesis for the origin of light-toned deposits (Baioni, 2013; Baioni & Wezel, 2010; Bishop et al., 2008; Flahaut et al., 2010; Fueten et al., 2014; Nedell, Squyres, & Anderson, 1987; Roach, Mustard, Swayze, et al., 2010b; Weitz & Parker, 2000).

(11) Leakages (RSL, Recurring Slope Lineae) were mapped on slopes of a northern sapping channel that denote very recent brine flows. RSLs were identified in Melas and Coprates Chasmata, but not in Ius Chasma (McEwen et al., 2014).

(12) This map is also the first which contains the full inventory of dune fields and impact craters in one of the Valles Marineris chasmata at decameter scale. There are 10,352 individual dune fields in Ius Chasma, covering together an area of 4753 km^2, and 49,452 impact craters displaying diameters from a few meters to 2902 m. Smaller craters were not visible due to the insufficient image resolution.

The interpretations presented here reflect the views of the authors, but are non-unique. For instance, chasma-bounding scarps observed below trimlines were interpreted as fault scarps in Peulvast et al. (2001). Mège and Bourgeois (2011) explained the shortcomings of the fault scarp interpretation, and suggested that faults parallel to the scarps guided the currently observed morphology, but did not keep their own geomorphological expression due to intense geomorphological reworking. Gourronc et al. (2014) showed that scarps interpreted as trimlines in Ius Chasma are widespread in other Valles Marineris chasmata. As trimlines are an element of a geomorphological system that includes many other glacial landforms, some morphologies interpreted on this map for which other interpretations could be proposed have also been interpreted as probably of glacial origin. For example, some chaotic or sandy areas that perfectly match the glacial interpretation were interpreted as glacial, even though other genetic interpretations are possible in alternative settings. By proceeding this way, the proposed landform interpretations are self-consistent and provide a coherent cartographic product.

As a consequence, the interpretations provided with this map, including in the map legend, reflect the current views of the authors.

5. Conclusions

The detailed investigation using CTX image mosaics, coupled with literature review and incorporating additional imagery and topographic data, led to the preparation of the first geomorphological map of Ius Chasma, which shows in detail one of the most complex Valles Marineris chasmata. The trough displays a huge diversity of landforms oproduced by tectonic, magmatic, mass movement, water-related, glacial, eolian, and impact cratering processes and events. Their number and spatial relationships have great potential for refining existing geomorphological and geological interpretations of Ius Chasma. Landslide scars are dominant landforms on the northern chasma

wall, while the southern slope of Ius Chasma predominantly contains spur-and-gully morphology walls and large sapping channel systems. The western end of the trough is filled with glacial deposits, whereas the central chasma part displays glacial features of erosional origin. Bright-toned sediments produced in a lacustrine environment, especially visible in the southern Ius graben, are masked by landslide deposits in most parts of the northern graben. Apart from well-defined units, the map also presents several object types which have not been reported and/or interpreted before (alluvial fans, RSLs, highly degraded landslide deposits, moraines, and other glacial landforms), and offers a view of dune fields, impact craters, and light-toned deposits in unprecedented detail. The map significantly helps clarify the role of geomorphological agents and processes along the entire Ius Chasma.

Acknowledgements

The authors thank Dr Olga Kromuszczyńska for her support, time, and commitment in the manuscript and map preparation.

Disclosure statement

No potential conflict of interest was reported by the authors.

Funding

This work was supported by the Foundation for Polish Science [project FNP TEAM/2011-7/9 "Mars: another planet to approach geoscience issues"].

ORCID

Krzysztof Dębniak http://orcid.org/0000-0002-4572-3144
Daniel Mège http://orcid.org/0000-0003-4304-9878
Joanna Gurgurewicz http://orcid.org/0000-0001-9792-3220

References

Andrews-Hanna, J. C. (2012). The formation of Valles Marineris: 2. Stress focusing along the buried dichotomy boundary. *Journal of Geophysical Research*, *117*(E04009), 1–17. doi:10.1029/2011JE003954

Baioni, D. (2013). Morphology and geology of an interior layered deposits in the western Tithonium Chasma, Mars. *Planetary and Space Science*, *89*, 140–150. doi:10.1016/j.pss.2013.09.019

Baioni, D., & Wezel, F. C. (2010). Morphology and origin of an evaporitic dome in the eastern Tithonium Chasma, Mars. *Planetary and Space Science*, *58*, 847–857. doi:10.1016/j.pss.2010.01.009

Banerdt, W. B., & Golombek, M. P. (2000). *Tectonics of the Tharsis region on Mars: Insights from the MGS topography and gravity*. 31st Lunar and Planetary Science Conference, 2038.pdf.

Bishop, J. L., Parente, M., Weitz, C. M., Noe Dobrea, E. Z., Calvin, W. M., Milliken, R. E., … CRISM Team. (2008). *Characterization of light-toned sulfate and hydrated silica layers at Juventae Chasma using CRISM, OMEGA, HiRISE and context images*. 39th Lunar and Planetary Science Conference, 2334.pdf.

Blasius, K. R., Cutts, J. A., Guest, J. E., & Masursky, H. (1977). Geology of the Valles Marineris; First analysis of imaging from the Viking I Orbiter primary mission. *Journal of Geophysical Research*, *82*(28), 4067–4091. doi:10.1029/JS082i028p04067

Brunetti, M. T., Guzzetti, F., Cardinali, M., Fiorucci, F., Santangelo, M., Mancinelli, P., … Borselli, L. (2014). Analysis of a new geomorphological inventory of landslides in Valles Marineris, Mars. *Earth and Planetary Science Letters*, *405*, 156–168. doi:10.1016/j.epsl.2014.08.025

Carr, M. H., & Head III, J. W. (2010). Geologic history of Mars. *Earth and Planetary Science Letters*, *294*, 185–203. doi:10.1016/j.epsl.2009.06.042

Chojnacki, M., Burr, D. M., & Moersch, J. E. (2014). Valles Marineris dune fields as compared with other Martian populations: Diversity of dune compositions, morphologies, and thermophysical properties. *Icarus*, *230*, 96–142. doi:10.1016/j.icarus.2013.08.018

Chojnacki, M., Burr, D. M., Moersch, J. E., & Wray, J. J. (2014). Valles Marineris dune sediment provenance and pathways. *Icarus*, *232*, 187–219. doi:10.1016/j.icarus.2014.01.011

Chojnacki, M., & Hynek, B. M. (2008). Geological context of water-altered minerals in Valles Marineris, Mars. *Journal of Geophysical Research*, *113*(E12005), 1–38. doi:10.1029/2007JE003070

Chojnacki, M., Moersch, J. E., & Burr, D. M. (2010). Climbing and falling dunes in Valles Marineris, Mars. *Geophysical Research Letters*, *37*(L08201), 1–7. doi:10.1029/2009GL042263

Christensen, P. R., Engle, E., Anwar, S., Dickenshied, S., Noss, D., Gorelick, N., & Weiss-Malik, M. (2009). *JMARS - A planetary GIS*. American Geophysical Union, Fall Meeting 2009, abstract #IN22A-06.

Craddock, R. A., & Howard, A. D. (2002). The case for rainfall on a warm, wet early Mars. *Journal of Geophysical Research*, *107*(E11, 5111), 1–21. doi:10.1029/2001JE001505

Ebben, T. H., Bergstrom, J., Spuhler, P., Delamere, A., & Gallagher, D. (2007). Mission to Mars: The HiRISE camera on-board MRO. *Proceedings of SPIE, the International Society for Optical Engineering*, 6690, 66900B.1–66900B.22.

Environmental Systems Research Institute. (2011). *ArcGIS desktop: Release 10*. Redlands, CA: Author.

Flahaut, J., Quantin, C., Allemand, P., Thomas, P., & Le Deit, L. (2010). Identification, distribution and possible origins of sulfates in Capri Chasma (Mars), inferred from CRISM data. *Journal of Geophysical Research*, *115*(E11007), 1–10. doi:10.1029/2009JE003566

Flahaut, J., Quantin, C., Clenet, H., Allemand, P., Mustard, J. F., & Thomas, P. (2012). Pristine Noachian crust and key geologic transitions in the lower walls of Valles Marineris: Insights into early igneous processes on Mars. *Icarus*, *221*, 420–435. doi:10.1016/j.icarus.2011.12.027

Frey, H. V. (1979). Thaumasia: A fossilized early forming Tharsis uplift. *Journal of Geophysical Research*, *84*, 1009–1023. doi:10.1029/JB084iB03p01009

Fueten, F., Flahaut, J., Stesky, R., Hauber, E., & Rossi, A. P. (2014). Stratigraphy and mineralogy of Candor Mensa, West Candor Chasma, Mars: Insight into the geologic history of Valles Marineris. *Journal of Geophysical Research: Planets*, *119*, 331–354. doi:10.1002/2013JE004557

Gaddis, L. R., Anderson, J., Becker K., Becker, T., Cook, D., Edwards, K., … Robinson, M. (1997). *An overview of the integrated software for imaging spectrometers (ISIS)*. 28th Lunar and Planetary Conference. Retrieved from 1226.pdf.

Gourronc, M., Bourgeois, O., Mège, D., Pochat, S., Bultel, B., Massé, M., … Mercier, D. (2014). One million cubic kilometers of fossil ice in Valles Marineris: Relicts of a 3.5 Gy old glacial landsystem along the Martian equator. *Geomorphology*, *204*, 235–255. doi:10.1016/j.geomorph.2013.08.009

Higgins, C. G. (1982). Drainage systems developed by sapping on Earth and Mars. *Geology*, *10*, 147–152. doi:10.1130/0091-7613(1982)10<147:DSDBSO>2.0.CO;2

Jackson, M. P. A., Adams, J. B., Dooley, T. P., Gillespie, A. R., & Montgomery, R. D. (2011). Modeling the collapse of Hebes Chasma, Valles Marineris, Mars. *Geological Society of America Bulletin*, 1–32. doi:10.1130/B30307.1

Kochel, R. C., & Piper, J. F. (1986). Morphology of large Valles on Hawaii: Evidence for groundwater sapping and comparison with Martian valleys. *Journal of Geophysical Research*, *91*(B13), E175–E192. doi:10.1029/JB091iB13p0E175

Le Deit, L., Bourgeois, O., Mège, D., Hauber, E., Le Mouélic, S., Massé, M., … Bibring, J. P. (2010). Morphology, stratigraphy, and mineralogical composition of a layered formation covering the plateaus around Valles Marineris, Mars: Implications for its geological history. *Icarus*, *208*, 684–703. doi:10.1016/j.icarus.2010.03.012

Lucchitta, B. K. (1999). Geologic map of Ophir and Central Candor Chasmata (MTM-05072) of Mars, 1:502,000. This is a map sheet. In Atlas of Mars, 1:500,000 Geologic Series, U.S. Geological Survey, Map I-2568.

Lucchitta, B. K., McEwen, A. S., Clow, G. D., Geissler, P. E., Singer, R. B., Schultz, R. A., & Squyres, S. W. (1992). This is a chapter. In M. S. Matthews, H. H. Kieffer, B. M. Jakosky, & C. Snyder (Eds.), *Mars* (pp. 453–492). Tuscon, AZ: The University of Arizona Press.

Malin, M. C., Bell III, J. F., Cantor, B. A., Caplinger, M. A., Calvin, W. M., Clancy, R. T., … Wolff, M. J. (2007). Context camera investigation on board the Mars reconnaissance orbiter. *Journal of Geophysical Research*, *112* (E05S04), 1–25. doi:10.1029/2006JE002808

Mangold, N., Ansan, V., Masson, P., Quantin, C., & Neukum, G. (2008). Geomorphic study of fluvial landforms on the northern Valles Marineris plateau, Mars. *Journal of Geophysical Research*, *113*(E08009), 1–23. doi:10.1029/2007JE002985

Mangold, N., Quantin, C., Ansan, V., Delacourt, C., & Allemand, P. (2004). Evidence for precipitation on Mars from dendritic valleys in the Valles Marineris area. *Science*, *305*, 78–81. doi:10.1126/science.1097549

Masson, P. (1977). Structure pattern analysis of the Noctis Labyrinthus-Valles Marineris region of Mars. *Icarus*, *30*, 49–62. doi:10.1016/0019-1035(77)90120-8

McCauley, J. F. (1978). Geologic map of the Coprates Quadrangle of Mars, 1 :5,000,000. This is a map sheet. In R. M. Batson, P. M. Bridges, J. L. Inge, & S. Dwornik (Eds.), *Atlas of Mars* (pp. 1–146). U.S. Geological Survey, Geol. Ser. MC-18, Misc. Invest. Ser. Map 1-897. Washington, DC: NASA.

McEwen, A. S., Dunad, C. M., Mattson, S. S., Toigo, A. D., Ojha, L., Wray, J. J., … Thomas, N. (2014). Recurring slope lineae in equatorial regions of Mars. *Nature Geoscience*, *7*, 53–58. doi:10.1038/ngeo2014

McEwen, A. S., Eliason, E. M., Bergstrom, J. W., Bridges N. T., Hansen, C. J., Delamere, W. A., … Weitz, C. M., (2007). Mar reconnaissance Orbiter's high resolution imaging science experiment (HiRISE). *Journal of Geophysical Research*, 112, E05S02. doi:10.1029/2005JE002605

Metz, J. M., Grotzinger, J. P., Mohrig, D., Milliken, R., Prather, B., Pirmez, C., … Weitz, C. M. (2009). Sublacustrine depositional fans in Southwest Melas Chasma. *Journal of Geophysical Research*, *114*(E10002), 1–17. doi:10.1029/2009JE003365

Metz, J. M., Grotzinger, J. P., Okubo, C., & Milliken, R. (2010). Thin-skinned deformation of sedimentary rocks in Valles Marineris, Mars. *Journal of Geophysical Research*, *115* (E11004), 1–28. doi:10.1029/2010JE003593

Mège, D., & Bourgeois, O. (2011). Equatorial glaciations on Mars revealed by gravitational collapse of Valles Marineris wallslopes. *Earth and Planetary Science Letters*, *310*, 182–191. doi:10.1016/j.epsl.2011.08.030

Mège, D., & Masson, P. (1996a). A plume tectonics model for the Tharsis province, Mars. *Planetary and Space Science Journal*, *44*, 1499–1546. doi:10.1016/S0032-0633(96)00113-4

Mège, D., & Masson, P. (1996b). Amounts of crustal stretching in Valles Marineris, Mars. *Planetary and Space Science Journal*, *44*, 749–781. doi:10.1016/0032-0633(96)00013-X

Nedell, S. S., Squyres, S. W., & Anderson, D. W. (1987). Origin and evolution of the layered deposits in the Valles Marineris, Mars. *Icarus*, *70*, 409–441. doi:10.1016/0019-1035(87)90086-8

Okubo, C. H. (2010). Structural geology of Amazonian-aged layered sedimentary deposits in southwest Candor Chasma, Mars. *Icarus*, *207*, 210–225. doi:10.1016/j.icarus.2009.11.012

Okubo, C. H., Lewis, K. W., McEwen, A. S., & Kirk, R. L. (2008). Relative age of interior layered deposits in southwest Candor Chasma based on high-resolution structural mapping. *Journal of Geophysical Research*, *113*(E12002), 1–15. doi:10.1029/2008JE003181

Pelkey, S. M., Jakosky, B. M., & Christensen, P. R. (2003). Surficial properties in Melas Chasma Mars, from Mars Odyssey THEMIS data. *Icarus*, *165*, 68–89. doi:10.1016/S0019-1035(03)00152-0

Peulvast, J. P. (1991). *Geomorphological map of Mars: Melas Chasma, 1:500,000*. Meudon: Laboratoire de géographie physique - ATP de planétologie INSU.

Peulvast, J. P., & Masson, P. L. (1993a). Melas Chasma: Morphology and tectonic patterns in central Valles Marineris (Mars). *Earth, Moon and Planets*, *61*, 219–248. doi:10.1007/BF00572246

Peulvast, J. P., & Masson, P. L. (1993b). Erosion and tectonics in central Valles Marineris (Mars): A new morpho-structural model. *Earth, Moon and Planets*, *61*, 191–217. doi:10.1007/BF00572245

Peulvast, J. P., Mège, D., Chiciak, J., Costard, F., & Masson, P. L. (2001). Morphology, evolution and tectonics of Valles Marineris wallslopes (Mars). *Geomorphology*, *37*, 329–352. doi:10.1016/S0169-555X(00)00085-4

Quantin, C., Allemand, P., & Delacourt, C. (2004). Morphology and geometry of Valles Marineris landslides. *Planetary and Space Science*, *52*, 1011–1022. doi:10.1016/j.pss.2004.07.016

Quantin, C., Allemand, P., Mangold, N., & Delacourt, C. (2004). Ages of Valles Marineris (Mars) landslides and implications for canyon history. *Icarus*, *172*, 555–572. doi:10.1016/j.icarus.2004.06.013

Quantin, C., Allemand, P., Mangold, N., Dromart, G., & Delacourt, C. (2005). Fluvial and lacustrine activity on layered deposits in Melas Chasma, Valles Marineris,

Mars. *Journal of Geophysical Research*, *110*(E12S19), 1–18. doi:10.1029/2005JE002440

Roach, L. H., Mustard, J. F., Lane, M. D., Bishop, J. L., & Murchie, S. L. (2010). Diagenetic haematite and sulfate assemblages in Valles Marineris. *Icarus*, *207*, 659–674. doi:10.1016/j.icarus.2009.11.029

Roach, L. H., Mustard, J. F., Swayze, G., Milliken, R. E., Bishop, J. L., Murchie, S. L., & Lichtenberg, K. (2010). Hydrated mineral stratigraphy of Ius Chasma, Valles Marineris. *Icarus*, *206*, 253–268. doi:10.1016/j.icarus.2009.09.003.

Schultz, R. A. (1995). Gradients in extension and strain at Valles Marineris, Mars. *Planetary and Space Science*, *43* (12), 1561–1566. doi:10.1016/0032-0633(95)00111-5.

Schultz, R. A. (1998). Multiple-process origin of Valles Marineris basins and troughs, Mars. *Planetary and Space Science*, *46*(6/7), 827–834. doi:10.1016/S0032-0633(98)00030-0.

Schultz, R. A. (2000). Fault-population statistics at the Valles Marineris extensional province, Mars: Implications for segment linkage, crustal strains, and its geodynamical development. *Tectonophysics*, *316*, 169–193. doi:10.1016/S0040-1951(99)00228-0

Scott, D. H., & Tanaka, K. L. (1986). *Geologic map of the western equatorial region of Mars, 1:15 000 000*. U.S. Geological Survey Misc. Invest. Ser., Map I-1802-A.

Sharp, R. P., & Malin, M. C. (1975). Channels on Mars. *Bulletin of the Geological Society of America*, *86*, 593–609.

Smith, D. E., Zuber, M. T., Frey, H. V., Garvin, J. B., Head, J.W., Muhleman, D. O., … Sun, X. (2001). Mars Orbiter LaserAltimeter – Experiment summary after the first year of global mapping of Mars. *Journal of Geophysical Research*, 106(E10), 23689–23722.

Tanaka, K. L., Skinner, J. A., Dohm, J. M., Irwin III, R. P., Kolb, E. J., Fortezzo, C. M., … Hare, T. M. (2014). *Geologic map of Mars, 1:20,000,000*. U.S. Geological Survey, Scientific Investigation Map 3292.

Weitz, C. M., Milliken, R. E., Grant, J. A., McEwen, A. S., Williams, R. M. E., Bishop, J. L., & Thomson, B. J. (2010). Mars Reconnaissance Orbiter observations of light-toned layered deposits and associated fluvial landforms on the plateaus adjacent to Valles Marineris. *Icarus*, *205*, 73–102. doi:10.1016/j.icarus.2009.04.017

Weitz, C. M., and Parker, T. J. (2000). *New evidence that the Valles Marineris interior layered deposits formed in standing bodies of water*. 31st Lunar and Planetary Science Conference, 1693.pdf.

Wendt, L., Gross, C., Kneissl, T., Sowe, M., Combe, J. P., Le Deit, L., … Neukum, G. (2011). Sulfates and iron oxides in Ophir Chasma, Mars, based on OMEGA and CRISM observations. *Icarus*, *213*, 86–103. doi:10.1016/j.icarus.2011.02.013

William, D. R. (2016). *Viking mission to Mars*. Retrieved from nssdc.gsfc.nasa.gov/planetary/viking.html

Witbeck, N. E., Tanaka, K. L., & Scott, D. H. (1991). Geologic map of the Valles Marineris region, Mars, 1:2,000,000. This is a map sheet. In Atlas of Mars, 1:2,000,000 Geologic Series, U.S. Geological Survey, Map I-2010.

Zuber, M. T., Smith, D. E., Solomon, S. C., Muhleman, D. O., Head, J. W., Garvin, J. B., … Bufton, J. L. (1992). The Mars Observer laser altimeter investigation. *Journal of Geophysical Research*, *97*, 7781–7797.